DOI: 10.1002/ejic.200600010

Rare Earth Benzotriazolates: Coordination Polymers Incorporating Decomposition Products from Ammonia to 1,2-Diaminobenzene in $^1_\infty[Ln(Btz)_3(BtzH)]$ (Ln = Ce, Pr), $^1_\infty[Ln(Btz)_3\{Ph(NH_2)_2\}]$ (Ln = Nd, Tb, Yb), and $^1_\infty[Ho_2(Btz)_6(BtzH)(NH_3)]$[‡]

Klaus Müller-Buschbaum,*[a] and Yassin Mokaddem[a]

Keywords: Solvent-free synthesis / Lanthanides / Benzotriazolate / Crystal structure / X-ray diffraction

The solvent-free melt reactions of benzotriazole (BtzH, $C_6H_4N_2NH$) with rare earth metals result in three different types of benzotriazolate coordination polymers. Early 4f metals yield $^1_\infty[Ln(Btz)_3(BtzH)]$ [Ln = Ce (**1**), Pr (**2**)], from neodymium to ytterbium the type $^1_\infty[Ln(Btz)_3\{Ph(NH_2)_2\}]$ is observed [Ln = Nd (**3**), Tb (**4**), Yb (**5**)], whereas the late 4f metal Ho gives $^1_\infty[Ho_2(Btz)_6(BtzH)(NH_3)]$ (**6**). Depending on the reaction conditions and the respective rare earth element, ligand fragments originating from decomposition products are incorporated in the coordination polymers. Compounds **1**–**3** and **6** were obtained as single crystals and their crystal structures determined by single-crystal X-ray analysis, whilst **4** and **5** were obtained as powders. X-ray powder diffraction shows the isotypic character of polymers **3**, **4**, and **5**. The benzotriazolates contain trivalent lanthanide ions with complete nitrogen coordination. Decomposition of the ligand accompanies the formation of the coordination polymers. X-ray analysis was combined with thermal analysis and mass spectrometry to investigate the influence of reaction temperatures on ligand decomposition. Ln-benzotriazolates exhibit aspects of materials science such as luminescence {$^5D_4 \rightarrow {}^7F_J$, J = 4–6 for $^1_\infty[Tb(Btz)_3\{Ph(NH_2)_2\}]$ (**4**)} without quenching by concentration.

Introduction

Nearly all syntheses in coordination chemistry, including rare earth chemistry, are carried out in solution, mostly in classical solvents such as THF, toluene, DME etc.[1–7] These syntheses are used to form a range of complexes, from the first cyclopentadienyl complexes[8] and metallocenes[9] to the oxo and amido complexes of today.[1–7] In contrast solvent-free syntheses by high-temperature reactions have been successfully utilized to obtain organic amides of the rare earth elements over the past seven years.[10–20] It has been shown that novel coordination chemistry is possible without classical solvent procedures. The products obtained from the extreme conditions of melt reactions are unique and exhibit interesting features such as the formation of homoleptic compounds[10–16] and coordination polymers,[10,16,17,19,20] whereas for syntheses in solvents, ligand criteria such as multi-chelating[21–27] are necessary to obtain homoleptic complexes. The reactivity of rare earth metals has proven to be high enough so that they can directly react with amine melts without the need for multi-chelation or high steric congestion. We have systematically developed this kind of solvent-free synthesis including the crystallization of products under the reaction conditions.[9,12–17,19,20] Independent from the synthesis, a systematic approach that involves the amine ligand leads from ammonia to unsubstituted and substituted 1-N heterocycles such as pyrrole[28–32] and carbazole,[16,20] to 2-N ligands such as imidazole[33] and pyrazole,[11,12,17,19] and to ring systems that contain three or more nitrogen atoms per ring. The tendency to release N_2 upon heating N-heterocycles increases as the number of N atoms they contain increases. It becomes exothermic for triazoles, whereas tetrazoles tend to become explosive.[34] Accordingly, high-temperature chemistry with these ligands is a synthetic challenge. 1*H*-Benzotriazole (BtzH) marks the first step in our approach as it is thermally more stable than one-ring 3-N ligands. Nonetheless, our results (**1**–**6**) already illustrate the influence of thermal decomposition on this chemistry. To the best of our knowledge no benzotriazolates of the rare earth elements have been previously known.

Results and Discussion

The solvent-free ampoule reactions of cerium, praseodymium, neodymium, terbium, holmium, and ytterbium with 1*H*-benzotriazole were carried out in the amine melt. The reactions with cerium and praseodymium yield single crystals of $^1_\infty[Ln(Btz)_3(BtzH)]$ (**1**, **2**) [Equation (1)], whereas

[‡] Btz^-: benzotriazolate anion, $C_6H_4N_3^-$; BtzH: benzotriazole, $C_6H_4N_2NH$

[a] Institut für Anorganische Chemie, Universität zu Köln, Greinstrasse 6, 50939 Köln, Germany
E-mail: Klaus.Mueller-Buschbaum@Uni-Koeln.DE

reactions with neodymium, terbium, holmium, and ytterbium metal result in compounds that contain additional ligands, 1,2-diaminobenzene and ammonia. Two different types are observed depending on the metal, $^1_\infty$[Ln(Btz)$_3${Ph(NH$_2$)$_2$}] for Ln = Nd (**3**), Tb (**4**), and Yb (**5**) [Equation (2)], and $^1_\infty$[Ln$_2$(Btz)$_6$(BtzH)(NH$_3$)] for Ln = Ho (**6**) [Equation (3)].

$$\text{Ln} + 4\ \text{H–Btz} \xrightarrow{\Delta T} {}^1_\infty[\text{Ln(Btz)}_3\text{(BtzH)}] + \text{H}_2 \quad (1)$$

$$\text{Ln} + 4\ \text{H–Btz} \xrightarrow{\Delta T} {}^1_\infty[\text{Ln(Btz)}_3\{\text{Ph(NH}_2)_2\}] + \tfrac{1}{2}\ \text{N}_2 \quad (2)$$

$$2\ \text{Ln} + 8\ \text{H–Btz} \xrightarrow{\Delta T} {}^1_\infty[\text{Ln}_2\text{(Btz)}_6\text{(BtzH)(NH}_3)] + \text{N}_2 + \text{H}_2 + \text{C}_6\text{H}_6 \quad (3)$$

Of the decomposition products of 1*H*-benzotriazole, both 1,2-diaminobenzene and ammonia are incorporated into the products and in the coordination spheres of the metal atoms, whilst the neutral molecules N_2, H_2, and benzene are not. Consequently, **6** was formed at the highest reaction temperatures used as Ho is the metal with the highest melting point in **1**–**6**. In order to illuminate this decomposition influence, we investigated the thermal behavior of 1*H*-benzotriazole and of the products of the syntheses.[35,36] It can be concluded that rare earth metals promote and induce the decomposition of BtzH by a redox reaction. With compound **5** a red phase is reproducibly formed in a ratio of 4:1, which probably contains Yb^{II} though this has not yet been confirmed as we have not succeeded in crystallizing it. In order to crystallize the products from Equation (2), solvothermal reaction and crystallization from pyrrole were carried out for **3**, whereas the melt synthesis results in powders to microcrystalline products as for **4** and **5**.

The thermal decomposition of each type of lanthanide benzotriazolates was investigated by simultaneous DTA/TG[37] on the bulk as well as on single crystalline materials of **1**, **3**, and **6**. This analysis provides additional information with regard to the completeness of the reactions, the possible phase impurities, and the decomposition path of the product of the melt reactions and the ligand used. We have already shown the value of this method for the comprehension of comparable melt reactions with 2,2-(pyridyl)benzimidazole, 2,2′-dipyridylamine, as well as with pyrazole.[10,14,38,39]

The DTA/TG versus temperature diagrams of the rare earth benzotriazolates presented here show an ensemble of endothermic as well as exothermic signals in the heat flow and are accompanied by several steps of mass losses, which end in the decomposition of the coordination polymers. Investigations of the bulk materials show additional signals that can be identified with excess ligand (BtzH: m.p. 98 °C, b.p. 204 °C, measured 95 °C, 205 °C). The diagram of the single crystalline material is free of these signals and exhibits the thermal processes of the products only (see Figure 1).

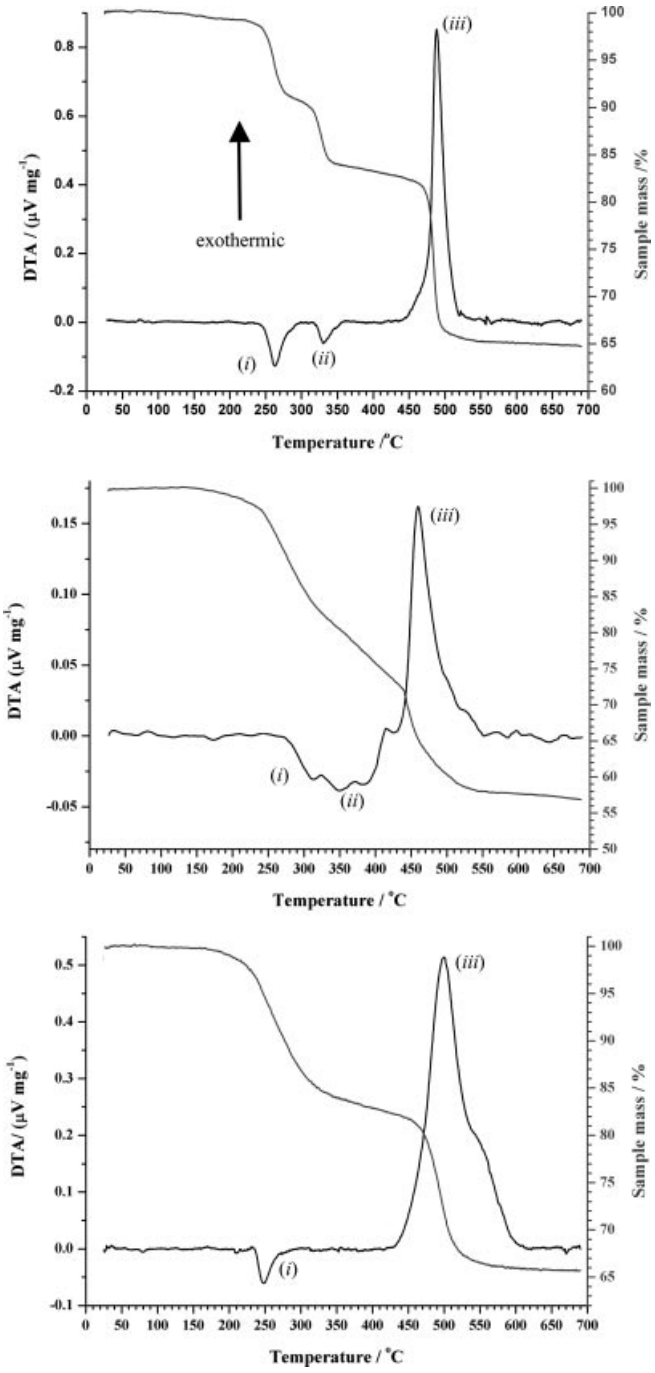

Figure 1. The thermal decompositions of $^1_\infty$[Ce(Btz)$_3$(BtzH)] (**1**, top), $^1_\infty$[Nd(Btz)$_3$(BtzH)] (**3**, middle) and $^1_\infty$[Ho$_2$(Btz)$_6$(BtzH)(NH$_3$)] (**6**, bottom), which were purified by sublimation. The compounds were investigated by simultaneous DTA/TG in the temperature range 20–700 °C. The release of amine ligands is observed first and is endothermic, whereas the decomposition of the amido backbone of the polymers is exothermic releasing N_2.

$^1_\infty$[Ce(Btz)$_3$(BtzH)] (**1**) releases coordinating benzotriazole in two endothermic steps at 250 °C and 320 °C [signals (*i*) and (*ii*)], which adds up to the mass loss of one equivalent of BtzH per formula (calculated 19%, observed 18%) and thus all coordinating BtzH. A strong exothermic peak [signal (*iii*)] follows at 470 °C, indicating decomposition of the

homoleptic polymer [Ce(Btz)$_3$] with the release of N_2. Furthermore, Ph(NH$_2$)$_2$, its decomposition products, and NH_3 can be observed in the mass spectrum.

Because of the different chemical formulas of $^1_\infty$[Nd(Btz)$_3${Ph(NH$_2$)$_2$}] (**3**) and **1**, differences in their simultaneous DTA/TG/MS **1** can be seen. Compound **3** shows a multistep decomposition with endothermic and exothermic signals but also three mass loss steps. At 270 °C [signal (*i*)], the release of coordinated Ph(NH$_2$)$_2$ begins [Ph(NH$_2$)$_2$: calculated 17.8%, observed 18%] before the polymer [Nd(Btz)$_3$] decomposes without a stable temperature plateau [310 °C: at least two steps, endothermic signal group (*ii*); 440 °C: exothermic step (*iii*)]. Prior to the exothermic release of N_2, Ph(NH$_2$)$_2$ as well as NH_3 are formed again from the coordinating Btz$^-$ anions.

$^1_\infty$[Ho$_2$(Btz)$_6$(BtzH)(NH$_3$)] (**6**) exhibits only two thermal decomposition steps. The first step at 240 °C [signal (*i*)] is, again, endothermic and can be identified with the release of the coordinated equivalent of BtzH and NH_3 (calculated 13.8%, observed 15.5%). Signal (*ii*) at 450 °C represents decomposition of [Ho(Btz)$_3$] accompanied by the release of the same products as for **1** and **3** (observed 17%).

It can thus be deduced that none of the coordination polymers melts congruently, that additional coordinating amine ligands in **1**–**6** are released prior to amide anions, and that the release of amide groups results in overall decomposition of the polymers. A general formula for a homoleptic decomposition intermediate is assumed to be [Ln(Btz)$_3$], though investigation of **3** shows that it is questionable to isolate these polymers for all lanthanide ions. Thermal stabilities of these coordination polymers are high, up to 450 °C for **5**. The exothermic release of N_2 is delayed to higher temperatures for **1**–**6** than for the free ligand.

Each of the far-infrared as well as Raman spectra of **1**–**6** show bands that cannot be identified with the ligand and thus represent the ν(Ln–N) and δ(N–Ln–N) stretching modes {$^1_\infty$[Ce(Btz)$_3$(BtzH)] (**1**) FarIR: 244, 200, 183, 169, Raman 123 cm^{-1}; $^1_\infty$[Pr(Btz)$_3$(BtzH)] (**2**) FarIR: 250, 195, 179, 171, Raman: 120 cm^{-1}; $^1_\infty$[Nd(Btz)$_3$(Ph(NH$_2$)$_2$)] (**3**) FarIR: 249, 195, 178, 147, Raman 150, 124 cm^{-1}; $^1_\infty$[Tb(Btz)$_3$(Ph(NH$_2$)$_2$)] (**4**) FarIR: 247, 193, 175, 146, Raman: 150 sh, 125 cm^{-1}; $^1_\infty$[Yb$_2$(Btz)$_6$(BtzH)(NH$_3$)] (**5**) FarIR: 254, 214, 173, 144 cm^{-1}; $^1_\infty$[Ho$_2$(Btz)$_6$(BtzH)(NH$_3$)] (**6**) FarIR: 249, 230, 210, 191, 176, 158, 146, Raman 122 cm^{-1}}. These bands match well with other Ln–N containing compounds like rare earth porphyrin complexes,[40] dipyridyl amides,[10,15,38] pyridylbenzimidazolates,[10,13,14] and carbazolates[10,16,20] with regard to the coordination spheres, valences, and ionic radii. Ligand lattice stretching modes are reflected by rather broad bands (FarIR: 423, 286 cm^{-1}). The MIR and Raman spectra additionally present vibrational bands of the benzotriazolate, diaminobenzene, and ammonia ligands, which are shifted by about ten wavenumbers relative to those of the free ligand, or show band splitting as a result of coordination to the metal centers and thus weakening of the C–N and C–C bonds. The ν(N–H) vibrational bands[41] of the amine ligands are also observed [**1**, **2**: BtzH: 3430 and 3422 cm^{-1}, respectively; **3**, **4**, **5**: Ph(NH$_2$)$_2$: 3360 and 3339, 3362 and 3333, 3363 and 3342 cm^{-1}, respectively; **6**: BtzH and NH_3: 3390 and 3367 cm^{-1}, respectively] and are confirmed by the MIR spectrum of the free ligands.[34] Furthermore, **3** shows a strong and broad band at 1975 cm^{-1} in the Raman spectrum according to the luminescence $^4I_{11/2}\rightarrow{}^4I_{9/2}$ for Nd^{III}[42] resulting from the frequency of the Nd-YAG laser of the IR-/Raman spectrometer.

The crystal structures of **1**–**6** consist of structurally related one-dimensional coordination polymers. Benzotriazolate ligands connect the metal centers and are thus vital for the formation of the strands. The coordination spheres of the 4f ions contain N atoms only of both amido and amino character. No π coordination is observed. As the

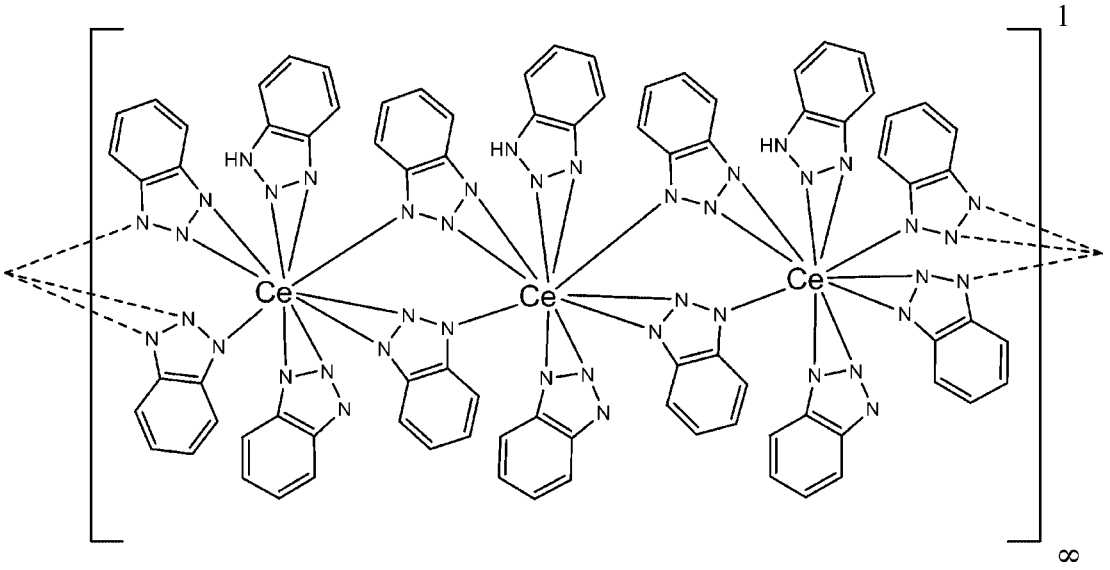

Scheme 1. μ-η^2;η^1- and η^2 coordination of the benzotriazolate and 1*H*-benzotriazole ligands in the coordination polymer $^1_\infty$[Ce(Btz)$_3$(BtzH)] (**1**). Pr^{III} exhibits an identical coordination in **2**.

structure analyses of **1** and **2** show, four Btz^- anions link a cerium or praseodymium center with two adjacent metal cations in a μ-η^2;η^1 manner such that two nitrogen atoms of one ligand coordinate to one metal ion and the third to the next metal center (see Scheme 1). Another Btz^- anion and the coordinated BtzH molecule do not participate in the polymer backbone and are coordinated to a single cerium atom in an η^2 fashion; a hydrogen bond between the two noncoordinating N atoms is present. The η^2 coordination shows a slight asymmetry of 5–10 pm in the corresponding Ln–N distances of **1** and **2**. Despite an octahedral arrangement of ligands the C.N. is ten for each Ce/Pr. Figure 2 depicts a part of the polymeric structure of $^1_\infty$[Ln(Btz)$_3$(BtzH)] [Ln = Ce (**1**) and Pr (**2**)] and Figure 3 the unit cell of the crystal structure.

The backbone of polymer **3** is identical to that of **1**, the difference stems from coordinated 1,2-diaminobenzene ligands that replace the benzotriazole molecules (see Scheme 2). The diaminobenzene ligands coordinate in a η^1;η^1 manner, with no hydrogen bond to the noncoordinating N atom of the third benzotriazolate equivalent. Replacement of the BtzH ligand in **1** and **2** with a Ph(NH$_2$)$_2$ ligand neither changes the C.N. nor the coordination polyhedron for **3**–**5**. Figure 4 displays part of the polymeric structure of $^1_\infty$[Nd(Btz)$_3${Ph(NH$_2$)$_2$}] (**3**) and Figure 5 the unit cell of the crystal structure.

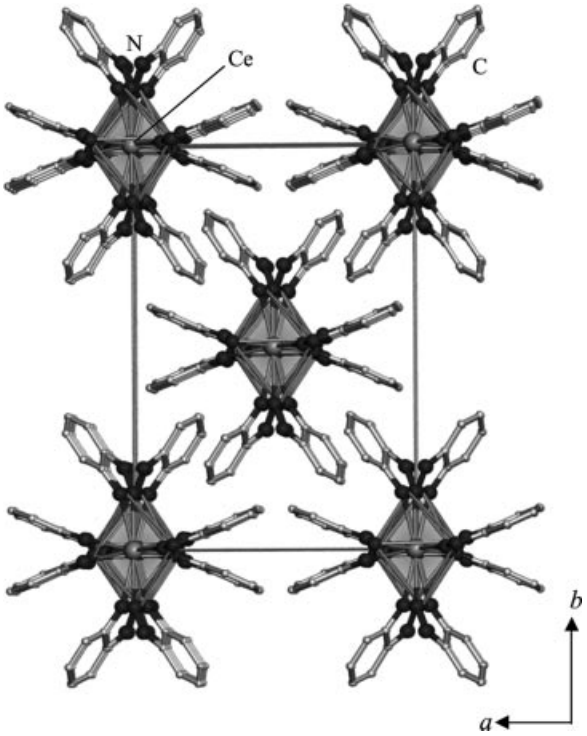

Figure 3. The crystal structure of $^1_\infty$[Ce(Btz)$_3$(BtzH)] (**1**) with a view along the chain direction [001]. N–N connection lines mark only the coordination polyhedra and not bonds.

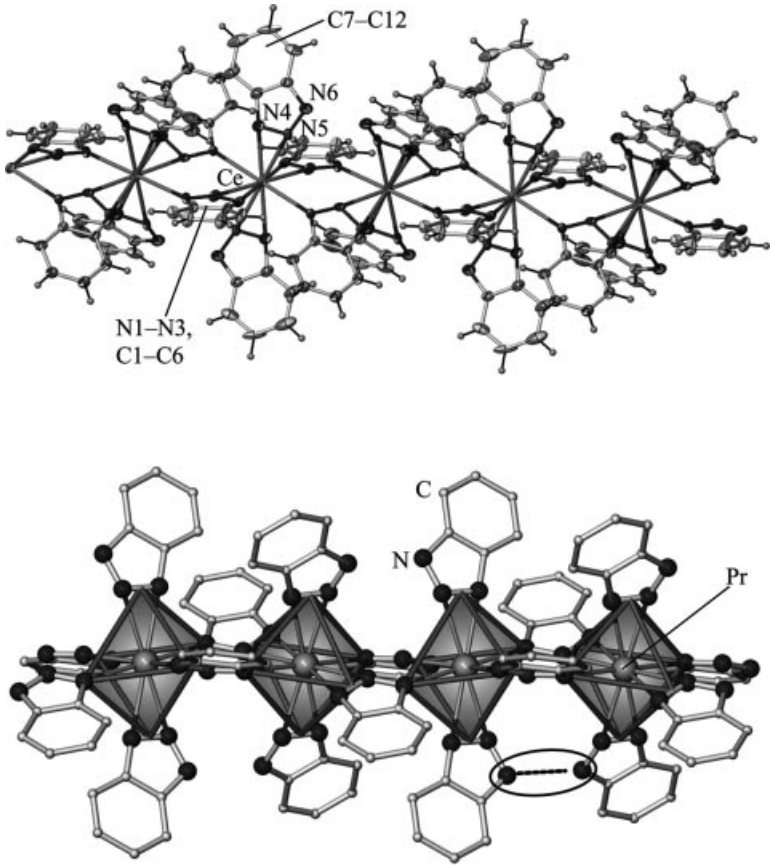

Figure 2. Section of the polymeric structure of $^1_\infty$[Ln(Btz)$_3$(BtzH)], Ln = Ce (**1**, top) and Pr (**2**, bottom). The hydrogen bond between the terminal Btz^- and BtzH ligands is represented by a dotted line. In this, and the following Figures, the thermal ellipsoids are scaled to a probability density level of the atoms of 50%. N–N connection lines mark only the coordination polyhedra and do not represent bonds. Metal atoms are depicted by large mid grey balls, nitrogen atoms by dark grey balls, and carbon atoms by small light grey balls.

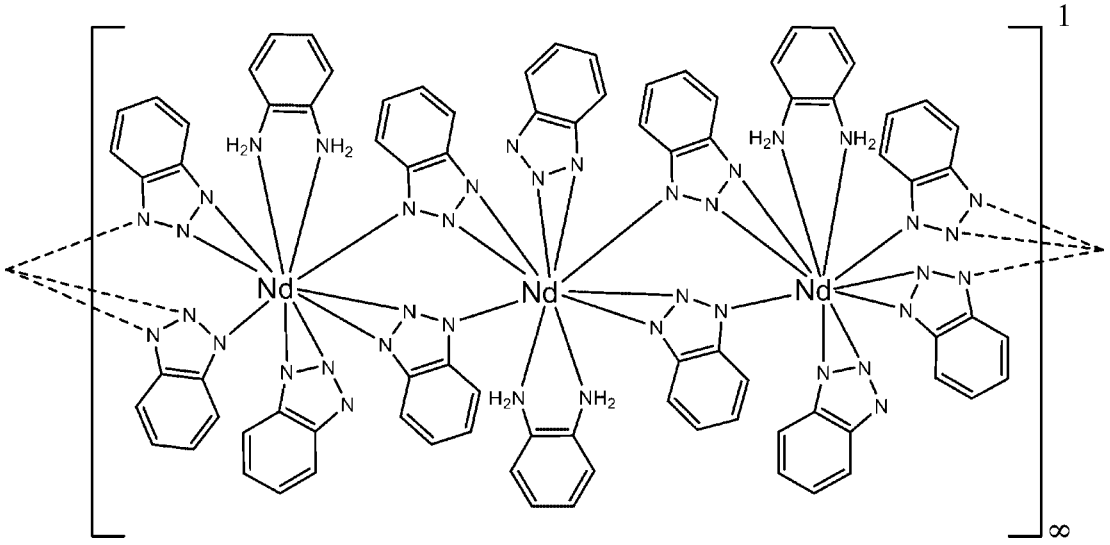

Scheme 2. μ-η^2;η^1- and η^1;η^1 coordination of the benzotriazolate and 1,2-diaminobenzene ligands in the coordination polymer $^1_\infty$[Nd(Btz)$_3${Ph(NH$_2$)$_2$}] (**3**). Tb^{III} and Yb^{III} exhibit identical polymers in **4** and **5**.

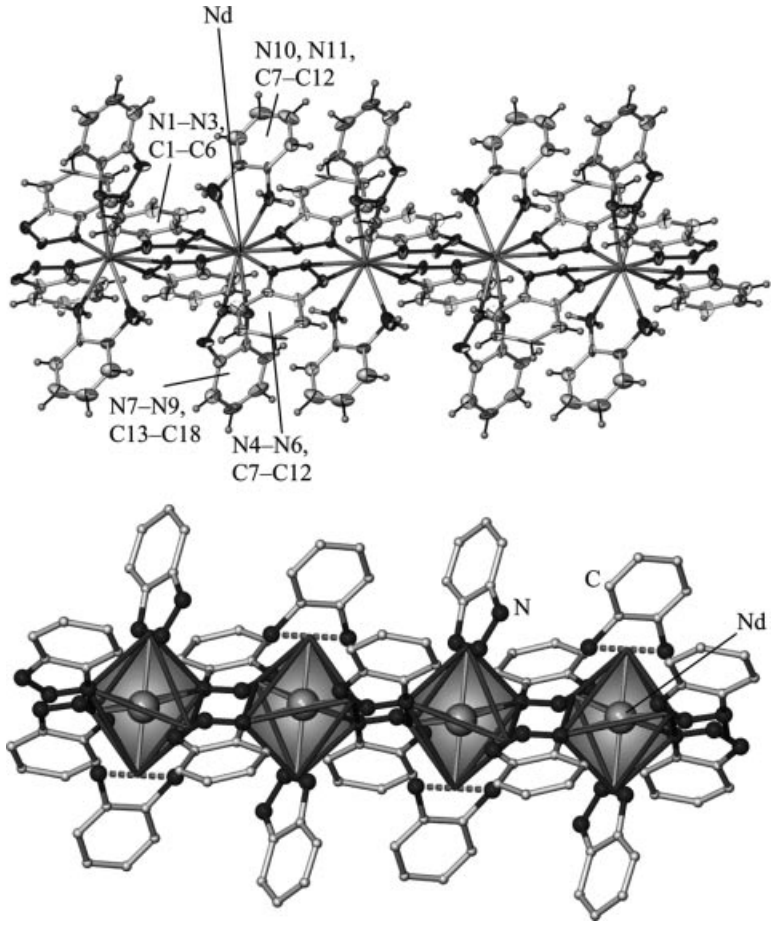

Figure 4. Section of the polymeric structure of $^1_\infty$[Nd(Btz)$_3${Ph(NH$_2$)$_2$}] (**3**) displaying thermal ellipsoids (top) and coordination polyhedra (bottom).

Polymer **6** differs from **1** and **3** in its backbone and additional ligands. The holmium ions are arranged in a triangular fashion that resembles a ladder-like structure (see Figure 6). No Ho–Ho bonds are observed in the triangles as benzotriazolate ligands again link the metal centers to build up a polymeric strand (see Scheme 3). Benzotriazole and ammonia molecules complete the coordination spheres of Ho. In contrast to **1**–**5**, the holmium polymer **6** exhibits

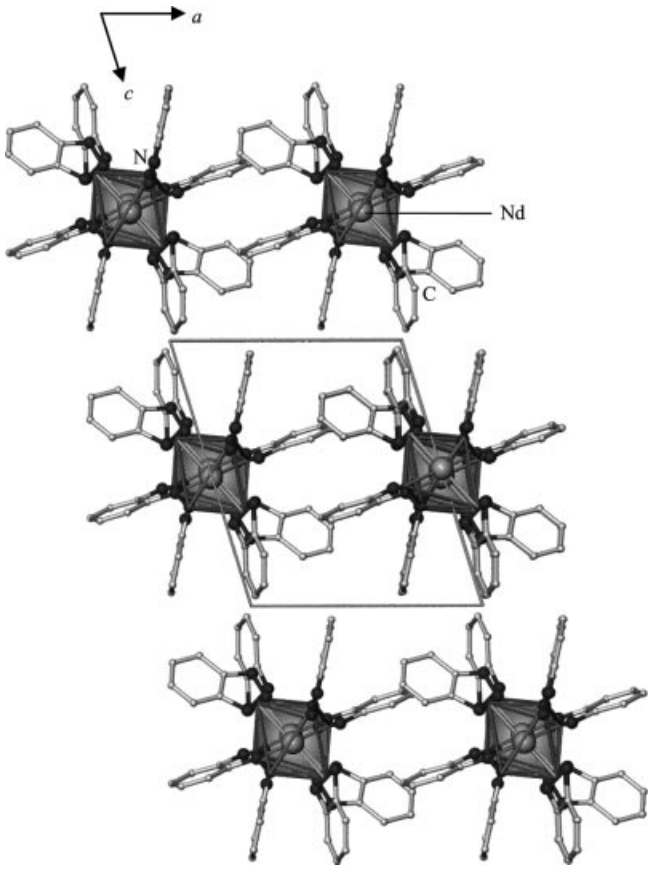

Figure 5. The crystal structure of $^{1}_{\infty}$[Nd(Btz)$_3${Ph(NH$_2$)$_2$}] (**3**) with a view along the chain direction [010]. The relation between the structures of the types $^{1}_{\infty}$[Ln(Btz)$_3${Ph(NH$_2$)$_2$}], Ln = Nd (**3**), Tb (**4**), Yb (**5**), and $^{1}_{\infty}$[Ln(Btz)$_3$(BtzH)], Ln = Ce (**1**), Pr (**2**), is evident.

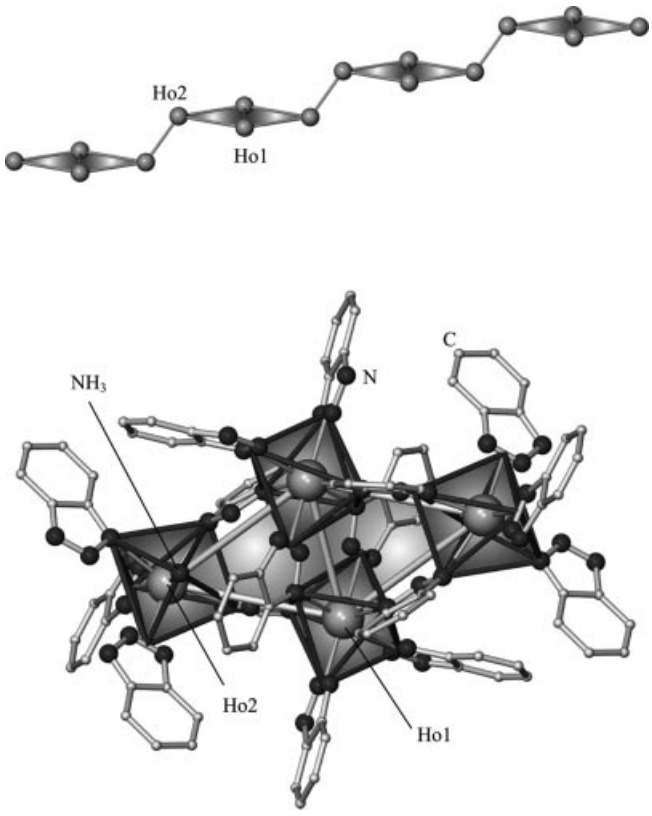

Figure 6. The arrangement of Ho atoms in **6** (top). Triangular units are combined to di-triangles with a common edge and form a ladder-like arrangement with no Ln–Ln bonds. The depiction at the bottom displays the ligands linking the metals to form double triangles. No triangular arrangement is observed for **1**–**5**.

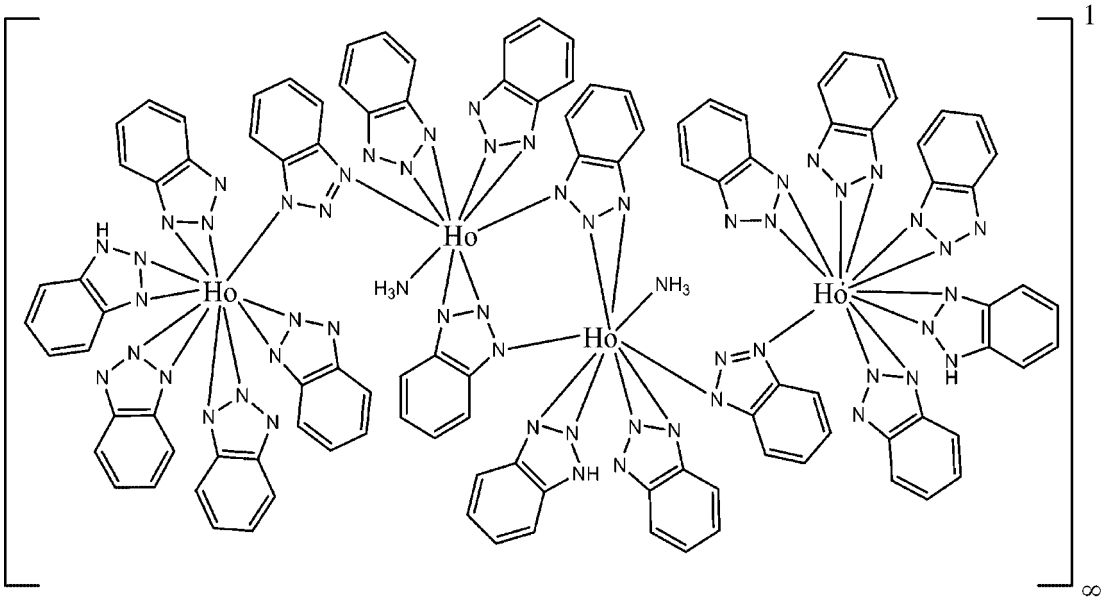

Scheme 3. μ-η^2:η^1-, η^2- and η^1:η^1 coordination of the benzotriazolate and 1*H*-benzotriazole ligands as well as the η^1 coordination of ammonia in polymeric $^{1}_{\infty}$[Ho$_2$(Btz)$_6$(BtzH)(NH$_3$)] (**6**).

a C.N. of 9 with two different holmium ions. Ho1 is surrounded by four μ-η^2;η^1 Btz^- ligands, one η^1;η^1 coordinated BtzH molecule, and one μ-(η^1;η^1) Btz^- anion that is linked to Ho2. Ho2 is also coordinated by four μ-η^2;η^1 Btz^- ligands, one μ-(η^1;η^1) Btz^- anion that is linked to Ho1, and one η^1-coordinated NH_3 molecule. Thus, one of the benzotriazolate ligands does not coordinate with its center nitrogen atom to any Ho atom. Two of the η^2-coordinated Btz^- anions show a strong asymmetry of >25 pm in their Ho–N distances, so that this coordination mode can also be referred to as μ-η^1;η^1;η^1. Figure 7 displays part of the polymeric structure of $^1_\infty[Ho_2(Btz)_6(BtzH)(NH_3)]$ (**6**) and Figure 8 the unit cell of the crystal structure.

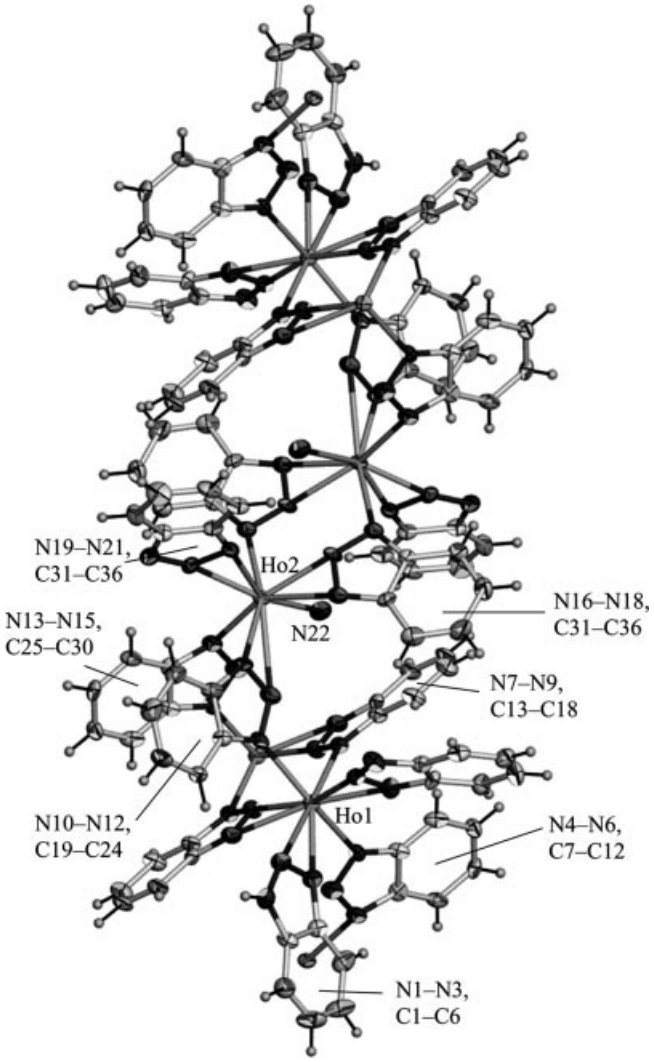

Figure 7. Part of the polymeric structure of $^1_\infty[Ho_2(Btz)_6(BtzH)(NH_3)]$ (**6**) displaying thermal ellipsoids (top) and coordination polyhedra (bottom).

The contraction of the radii of the lanthanide ions[43] influences both the C.N. as well as the Ln–N distances and is observed throughout the course of the products. In general, the C.N.s are high also for lanthanides, which mainly derives from the η^1;η^1 mode of the coordinated neighboring N atoms of the ligands. All rare earth ions are trivalent in

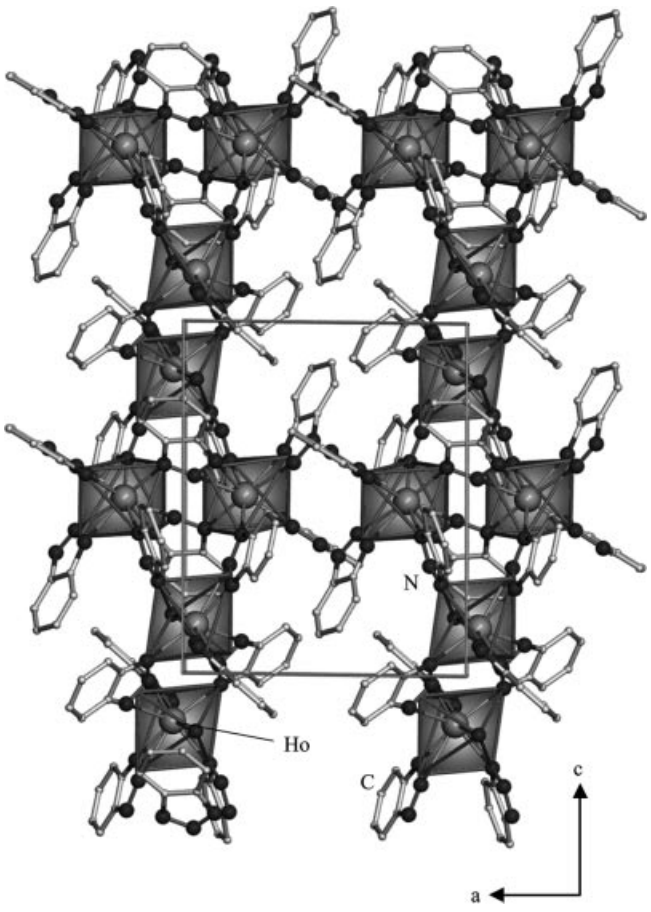

Figure 8. The crystal structure of $^1_\infty[Ho_2(Btz)_6(BtzH)(NH_3)]$ (**6**) with a view on the chains along [010].

1–**6**. The Ln–N distances range from 232.6(9)–253(1) pm for Ho–N amide and amine distances, to 248(2)–264(2) pm for Nd, through to 251.6(9)–265.0(9) pm for Ce. These distances match well with those of other trivalent lanthanide amido and amino complexes in which the metal ions are linked such as dipyridylamides $[Ln_2(Dpa)_6]$, Dpa^- = $(C_5H_4N)_2N^-$, with 236–255 pm for Ho^{III}, 244–268 pm for Nd^{III}, and 247–273 pm for Ce^{III}.[38] For a detailed selection of interatomic distances and angles see Table 1. Deviations of the coordination polyhedron from a regular octahedron are less than five degrees for all metal ions.

Powder diffraction of $^1_\infty[Tb(Btz)_3\{Ph(NH_2)_2\}]$ (**4**) and $^1_\infty[Yb(Btz)_3\{Ph(NH_2)_2\}]$ (**5**) shows that the compounds crystallize in a manner isotypic to that of $^1_\infty[Nd(Btz)_3\{Ph(NH_2)_2\}]$ (**3**). Thus, the description of the crystal structure in the space group $P\bar{1}$ is analogous to that of **3**. According to the larger ionic radius of Nd^{III} than those of Tb^{III} and Yb^{III},[43] the unit cells of **4** and **5** are smaller than that of **3** {**3**: 1314.2(2), **4**: 1258.2(3), **5**: 1232(1) [$\times 10^6$ pm^3]}.

$^1_\infty[Tb(Btz)_3\{Ph(NH_2)_2\}]$ (**4**) exhibits a strong green emission when exposed to UV light. The luminescence can be identified with the emission processes of the Tb^{3+} ions $^5D_4 \rightarrow {}^7F_4$ at 590 nm, $^5D_4 \rightarrow {}^7F_5$ at 545 nm, and $^5D_4 \rightarrow {}^7F_6$ at 490 nm.[44,45] Though **4** contains 100% Tb and is not a doped compound, no quenching of the luminescence by

Table 1. Selected distances and angles for $^1_\infty$[Ce(Btz)$_3$(BtzH)] (**1**), $^1_\infty$[Pr(Btz)$_3$(BtzH)] (**2**), $^1_\infty$[Nd(Btz)$_3${Ph(NH$_2$)$_2$}] (**3**), and $^1_\infty$[Ho$_2$(Btz)$_6$(BtzH)(NH$_3$)] (**6**). Deviations are given in brackets.

$^1_\infty$[Ce(Btz)$_3$(BtzH)] (**1**)		$^1_\infty$[Pr(Btz)$_3$(BtzH)] (**2**)	
Atoms	Distance [pm]	Atoms	Distance [pm]
Ce–N1	259(1)	Pr–N1	256.2(6)
Ce–N2	252.1(9)	Pr–N2	251.7(5)
Ce–N3[a]	265.3(9)	Pr–N3[a]	265.6(5)
Ce–N4	259.1(8)	Pr–N4	258.1(8)
Ce–N5	264.1(7)	Pr–N5	262.5(7)
Ce–Ce[a]	535.8(1)	Pr–Pr[a]	534.9(1)
N–C(range)	136(2)–138(2)	N–C(range)	135.3(9)–137.1(9)
N–N(range)	132(1)–135(1)	N–N(range)	132.8(8)–133.6(8)
Atoms	Angles [°]	Atoms	Angles [°]
N1–Ce–N2	30.2(3)	N1–Pr–N2	30.5(2)
N1–Ce–N3	102.1(3)	N1–Pr–N3	102.0(2)
N2–Ce–N4	86.5(4)	N2–Pr–N4	86.6(3)
N2–Ce–N5	102.4(3)	N2–Pr–N5	103.6(3)
N3–Ce–N2	74.0(3)	N3–Pr–N2	73.7(2)
N3–Ce–N5	97.4(3)	N3–Pr–N5	98.0(3)
N4–Ce–N5	29.1(3)	N4–Pr–N5	29.5(2)

$^1_\infty$[Nd(Btz)$_3${Ph(NH$_2$)$_2$}] (**3**)		$^1_\infty$[Ho$_2$(Btz)$_6$(BtzH)(NH$_3$)] (**6**)	
Atoms	Distance [pm]	Atoms	Distance [pm]
Nd–N1	262(2)	Ho1–N1	244(1)
Nd–N2	250(2)	Ho1–N2	279.5(8)
Nd–N3[b]	259(2)	Ho1–N4	245(1)
Nd–N4	258(2)	Ho1–N5	236.5(9)
Nd–N5[c]	250(2)	Ho1–N7	244.5(9)
Nd–N6[c]	257(2)	Ho1–N13	244.3(9)
Nd–N8	248(2)	Ho1–N14[d]	236.5(9)
Nd–N9	255(2)	Ho1–N15[d]	253(1)
Nd–N10	261(2)	Ho1–N18[d]	244.8(9)
Nd–N11	264(2)	Ho2–N8	283(1)
N–C(range)	136(2)–145(3)	Ho2–N9	234.4(9)
N–N(range)	132(2)–136(2)	Ho2–N10	232.6(9)
Nd–Nd[b]	521.6(1)	Ho2–N11	242.4(9)
Nd–Nd[c]	514.8(1)	Ho2–N16	241(1)
		Ho2–N19	249(1)
		Ho2–N20	241.2(9)
		Ho2–N21[e]	247.4(9)
		Ho2–N22	245.6(9)
		Ho1–Ho2	591.5(1)
		Ho1–Ho1[d]	493.6(1)
		Ho2–Ho2[e]	478.5(1)
		N–C(range)	134(2)–138(2)
		N–N(range)	132(1)–136(2)
Atoms	Angles [°]	Atoms	Angles [°]
N1–Nd–N2	30.1(4)	N1–Ho1–N4	86.7(4)
N1–Nd–N3	107.2(5)	N2–Ho1–N7	88.2(3)
N2–Nd–N4	101.6(5)	N5–Ho1–N13	99.8(3)
N5–Nd–N6	30.1(5)	N9–Ho2–N10	88.0(4)
N4–Nd–N5	78.5(6)	N11–Ho2–N16	89.6(3)
N8–Nd–N9	30.2(4)	N8–Ho2–N9	27.7(3)
N10–Nd–N11	63.3(5)	N19–Ho2–N22	78.8(4)

[a] $-x$, y, $-z + 1/2$. [b] $-x + 1$, $-y$, $-z + 1$. [c] $-x + 2$, $-y$, $-z + 1$. [d] $-x + 2$, $-y + 1$, $-z + 1$. [e] $-x + 2$, $-y + 1$, $-z$.

concentration is observed. The emission spectrum of **4**, and the absorption spectra of **4** (room temperature and 120 K) and 1*H*-benzotriazole (room temperature) can be seen in Figure 9. A comparison of the absorption spectra of the free ligand with that of polymer **4** shows excitation of the ligand into the Soret band in the UV region. Benzotriazole and its derivatives are commercially used as UV absorbers.[46,47] We assume an energy transfer from the ligand to the metal ions as the luminescence is present independent of whether the excited states of Tb or the ligand are populated; additionally both absorption maxima of $^1_\infty$[Tb(Btz)$_3${Ph(NH$_2$)$_2$}] (**4**) at 310 and 205 nm cannot be identified with Tb^{III} absorptions. We chose 310 nm as the excitation wavelength for the emission spectrum of **4**. Furthermore, an energy back-transfer from the metal centers to the ligand is possible, which would lead to quenching. Presently, we cannot explain why no quenching by concentration is observed. High resolution excitation spectra of **4** as well as of BtzH, emission efficiency, and decay time measurements are planned to further investigate the luminescence properties of $^1_\infty$[Tb(Btz)$_3${Ph(NH$_2$)$_2$}].

Conclusions

The formation of **1**–**6** shows that triazolates can also be utilized for high-temperature oxidations of rare earth metals with amines. Though the release of N_2 from BtzH is exothermic, coordination polymers of the 4f elements can be obtained below the decomposition temperature. Depending on the temperature and lanthanide, three chemically different polymers can be obtained. With the largest lanthanide ions and the lowest melt temperatures, $^1_\infty$[Ln(Btz)$_3$(BtzH)] is formed up to praseodymium. $^1_\infty$[Ln(Btz)$_3${Ph(NH$_2$)$_2$}] is formed from neodymium to ytterbium. $^1_\infty$[Ln$_2$(Btz)$_6$(BtzH)(NH$_3$)] has so far been isolated for holmium only, and at the highest reaction temperatures investigated. Compounds **1**–**6** are the first triazolates of the lanthanides. Partial decomposition of the benzotriazole ligands accompanies the syntheses and yields 1,2-diaminobenzene as well as ammonia, which are both incorporated in the coordination polymers of the heavier 4f elements. Thermal analyses of **1**, **3**, and **6** lead to the assumption that homoleptic polymers [Ln(Btz)$_3$] are formed upon release of the coordinated amine ligands, though these polymers could not be isolated as single crystalline material so far. The coordination polymers also exhibit aspects of materials science such as a green luminescence {$^5D_4 \rightarrow {}^7F_J$, J = 4–6 for $^1_\infty$[Tb(Btz)$_3${Ph(NH$_2$)$_2$}] (**4**)} without quenching by concentration, and an energy transfer from the ligand to the Tb^{3+} ions.

Experimental Section

All reactions were carried out under argon using a dry box and standard Schlenk and ampoule techniques because of the air- and moisture-sensitivity of **1**–**6**. The lanthanide metals (ChemPur, STREM, 99.9%) and 1*H*-benzotriazole (ACROS, 99%) were used

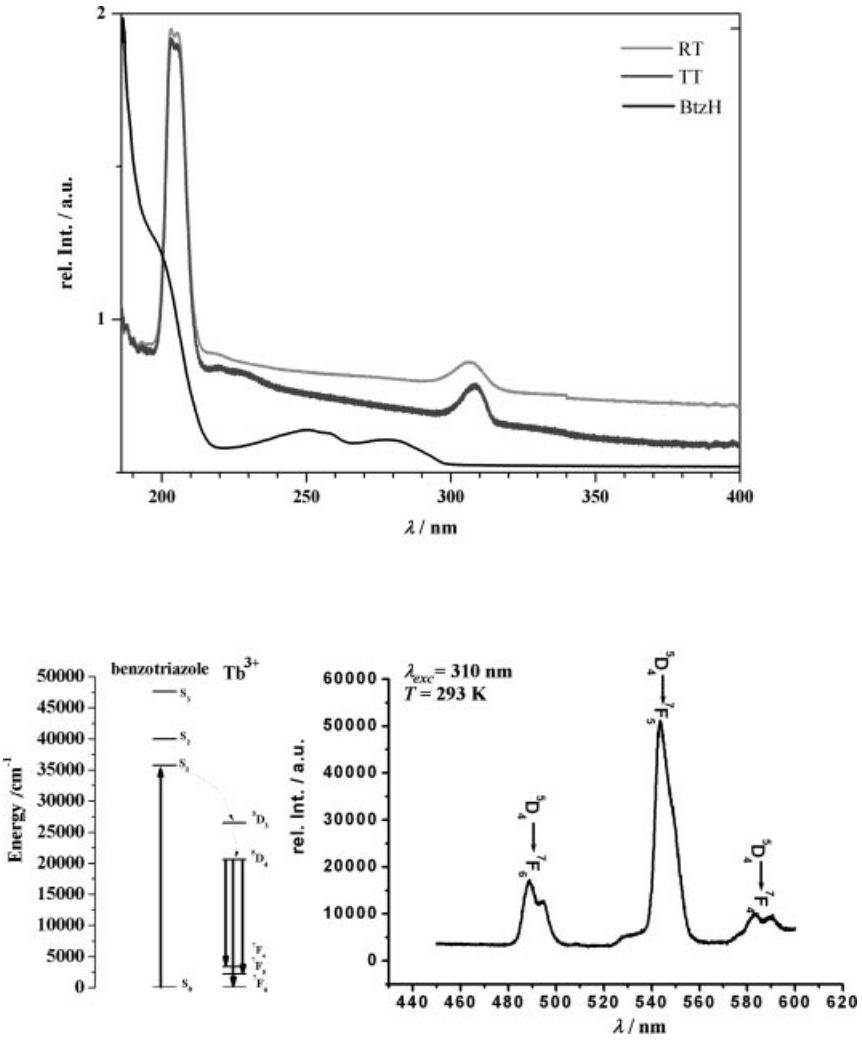

Figure 9. The absorption spectra of $^{1}_{\infty}$[Tb(Btz)$_3${Ph(NH$_2$)$_2$}] (**4**) at 293 and 120 K and that of 1*H*-benzotriazole at 293 K (top), and the emission spectrum of **4** with an excitation wavelength of λ = 310 nm (bottom).

as purchased. Mercury (Fluka, 99.9%) was used for activation of the metals. The IR spectra were recorded with a BRUKER FTIR-IS66V-S spectrometer, the Raman spectra with a BRUKER FRA 106-S spectrometer. For MIR investigations KBr pellets and for FIR measurements PE pellets were used under vacuum. The absorption spectroscopy was carried out at 293 and 120 K with a VARIAN Carey 05E (BRUKER) spectrometer on samples sealed under argon between CaF_2 windows. Emission spectroscopy was carried out with a SPEX-Flurolog DM3000F fluorescence spectrometer (JOBIN YVON GmbH) on samples sealed under vacuum in quartz tubes. The thermal decompositions of **1**, **3**, and **6** were studied using simultaneous DTA/TG (NETZSCH STA-409) on samples that were previously purified of excess BtzH and pyrrole by evaporation (16.1 mg of the Ce product **1**, 18.5 mg of the Nd product **3**, and 12.0 mg of the Ho product **6**). The samples were heated from 20–700 °C at a heating rate of 10 °C/min in a constant Ar flow of 60 mL/ min.

$^{1}_{\infty}$[Ce(Btz)$_3$(BtzH)] (1): Cerium metal (70 mg, 0.5×10^{-3} mol), the amine 1*H*-benzotriazole (BtzH, $C_6H_4N_2NH$; 179 mg, 1.5×10^{-3} mol), and Hg (20 mg) were sealed in an evacuated DURAN glass ampoule. The reaction mixture was heated over 5 h to 100 °C and over another 80 h to 140 °C. The temperature was held constant for 48 h. The melt was cooled down to 90 °C over 150 h and then to room temperature over 14 h. Except for a slight excess of Ce metal and BtzH, the reaction reached completion to give highly reflective colorless crystals of **1** (0.2–0.3 mm in size). Yield: 275 mg (91%). MIR: 3430 (m), 3343 (m), 3260 (m), 3076 (m), 1577 (m), 1502 (m), 1483 (m), 1444 (m), 1388 (w), 1280 (s), 1259 (m), 1208 (m), 1188 (s), 1143 (s), 1084 (m), 991 (m), 937 (m), 914 (s), 781 (vs), 753 (vssh), 744 (vs), 694 (m), 633 (s) cm^{-1}. FarIR: 551 (s), 438 (m), 420 (w), 286 (w), 244 (m), 200 (s), 183 (m), 169 (s), 101 (w) cm^{-1}. Raman: 3307 (w), 3247 (s), 3078 (w), 1575 (w), 1387 (m), 1283 (w), 1128 (w), 1020 (m), 782 (m), 631 (s), 123 (s), 100 (msh) cm^{-1}. $CeC_{24}H_{17}N_{12}$ (613.36): calcd. C 47.28, H 2.79, N 27.55; found C 47.8, H 3.0, N 27.6.

$^{1}_{\infty}$[Pr(Btz)$_3$(BtzH)] (2): Praseodymium metal (71 mg, 0.5×10^{-3} mol), the amine 1*H*-benzotriazole (BtzH, $C_6H_4N_2NH$; 179 mg, 1.5×10^{-3} mol), and Hg (20 mg) were sealed in an evacuated DURAN glass ampoule. The reaction mixture was heated over 18 h to 135 °C. The temperature was held constant for 672 h. The melt was cooled down to room temperature over 18 h. Except for a slight excess of Pr metal and BtzH, the reaction reached completion to give highly reflective greenish yellow crystals of **2** (0.05–0.15 mm in size). Yield: 260 mg (84%). MIR: 3422 (m), 3341 (m), 3135 (s), 1577 (w), 1502 (w), 1484 (w), 1442 (m), 1401 (vs), 1281 (m), 1259 (w), 1208 (w), 1175 (s), 1151 (m), 1085 (w), 1008 (w), 988 (w), 962

(w), 914 (m), 781 (s), 744 (vs), 694 (w), 633 (m) cm^{-1}. FarIR: 550 (m), 433 (w), 422 (w), 290 (w), 242 (w), 195 (m), 179 (m), 171 (m), 101 (w) cm^{-1}. Raman: 3216 (w), 3066 (m), 1574 (m), 1485 (w), 1442 (w), 1386 (s), 1283 (m), 1127 (m), 1020 (s), 783 (s), 633 (m), 551 (w), 120 (vssh), 110 (vs) cm^{-1}. $C_{24}H_{17}N_{12}Pr$ (614.24): calcd. C 46.91, H 2.77, N 27.34; found C 47.0, H 2.9, N 27.3.

$^1_\infty$[Nd(Btz)$_3${Ph(NH$_2$)$_2$}] (3): Neodymium metal (72 mg, 5×10^{-4} mol), pyrrole (503 mg, 7.5×10^{-3} mol), the amine 1*H*-benzotriazole (BtzH, $C_6H_4N_2NH$; 179 mg, 1.5×10^{-3} mol) together with Hg (20 mg) were frozen with liquid nitrogen, degassed, and sealed in an evacuated DURAN glass ampoule. The reaction mixture was heated over 4 h to 100 °C and over another 100 h to 150 °C. The temperature was held constant for 48 h. The reaction was cooled to 90 °C over 200 h and down to room temperature over 13 h. Except for the liquid pyrrole, the reaction reached completion to give reflective violet crystals of **3** (0.15–0.2 mm in size). Yield: 285 mg (94%). MIR: 3360 (m), 3338 (m), 3138 (s), 1593 (w), 1576 (m), 1484 (m), 1443 (m), 1400 (s), 1283 (m), 1259 (m), 1181 (s), 1150 (s), 1082 (m), 1010 (w), 989 (w), 942 (w), 914 (m), 848 (w), 781 (vs), 747 (vs), 696 (m), 633 (m) cm^{-1}. FarIR: 550 (m), 433 (w), 277 (w), 249 (w), 195 (m), 178 (m), 147 (w) cm^{-1}. Raman: 3067 (m), 1975 (vs), 1568 (w), 1386 (m), 1282 (w), 1127 (m), 1020 (m), 782 (m), 631 (w), 551 (w), 150 (vssh), 124 (vs) cm^{-1}. $C_{24}H_{20}N_{11}Nd$ (606.48): calcd. C 47.47, H 3.30, N 25.38; found C 48.0, H 3.3, N 25.5.

$^1_\infty$[Tb(Btz)$_3${Ph(NH$_2$)$_2$}] (4): Terbium metal (80 mg, 5×10^{-4} mol), the amine 1*H*-benzotriazole (BtzH, $C_6H_4N_2NH$; 179 mg, 1.5×10^{-3} mol) together with Hg (20 mg) were sealed in an evacuated DURAN glass ampoule. The reaction mixture was heated over 4 h to 100 °C and over another 120 h to 160 °C. The temperature was held constant for 240 h. The melt was cooled to 90 °C over 140 h and down to room temperature over 13 h. Except for a slight excess of the reactants, the reaction reached completion to give a reflective colorless microcrystalline material of **4**. Yield: 265 mg (85%). MIR: 3333 (w), 3146 (m), 3069 (m), 1593 (w), 1577 (m), 1487 (m), 1443 (m), 1400 (m), 1284 (m), 1259 (m), 1183 (s), 1167 (s), 1141 (m), 1008 (w), 990 (m), 942 (w), 915 (m), 781 (vs), 742 (vs), 694 (m), 634 (m) cm^{-1}. FarIR: 550 (s), 432 (m), 279 (w), 247 (w), 193 (m), 175 (m), 146 (w) cm^{-1}. Raman: 3066 (s), 1567 (m), 1442 (m), 1387 (s), 1285 (m), 1172 (w), 1127 (m), 1022 (s), 784 (s), 631 (m), 432 (w), 150 (mssh), 125 (vssh), 110 (vs) cm^{-1}. $C_{24}H_{20}N_{11}Tb$ (621.16): calcd. C 46.38, H 3.22, N 24.78; found C 46.0, H 2.8, N 25.1.

$^1_\infty$[Yb(Btz)$_3${Ph(NH$_2$)$_2$}] (5): Ytterbium metal (87 mg, 5×10^{-4} mol), the amine 1*H*-benzotriazole (BtzH, $C_6H_4N_2NH$; 179 mg, 1.5×10^{-3} mol), and Hg (20 mg) were sealed in an evacuated DURAN glass ampoule. The reaction mixture was heated over 4 h to 100 °C and over another 168 h to 150 °C. The temperature was held constant for 48 h. The melt was cooled to 90 °C over 200 h and down to room temperature over 13 h. Except for a slight excess of the reactants, the reaction gave reflective colorless microcrystalline material of **5** as well as an unknown, poorly crystalline, red material in a ratio of 4:1. Yield: 178 mg (60%). MIR: 3393 (w), 3342 (w), 3141 (m), 3065 (m), 1613 (w), 1570 (m), 1501 (w), 1487 (m), 1443 (m), 1390 (m), 1285 (s), 1258 (m), 1205 (s), 1175 (s), 1140 (m), 1129 (w), 1076 (w), 990 (m), 914 (m), 782 (vs), 742 (vs), 694 (m), 633 (s) cm^{-1}. FarIR: 552 (m), 431 (m), 279 (w), 254 (m), 214 (msh), 173 (msh), 148 (m) cm^{-1}. $C_{24}H_{20}N_{11}Yb$ (635.28): calcd. C 45.35, H 3.15, N 24.23; found C 44.9, H 3.1, N 24.1.

$^1_\infty$[Ho$_2$(Btz)$_6$(BtzH)(NH$_3$)] (6): Holmium metal (83 mg, 5×10^{-4} mol), the amine 1*H*-benzotriazole (BtzH, $C_6H_4N_2NH$; 179 mg, 1.5×10^{-3} mol), and Hg (20 mg) were sealed in an evacuated DURAN glass ampoule. The reaction mixture was heated over 8 h to 100 °C and over another 200 h to 180 °C. The melt was cooled without a temperature plateau to 90 °C over 100 h and down to room temperature over 24 h. Except for a slight excess of the reactants, the reaction reached completion to give pink crystals of **6** (0.15–0.2 mm in size). Yield: 280 mg (95%). MIR: 3367 (w), 3150 (m), 3073 (m), 1593 (w), 1502 (w), 1485 (m), 1444 (m), 1387 (w), 1285 (m), 1261 (m), 1207 (s), 1184 (s), 1149 (m), 1129 (w), 1009 (w), 989 (m), 915 (m), 782 (vs), 744 (vs), 695 (m), 634 (m) cm^{-1}. FarIR: 551 (m), 430 (m), 422 (m), 409 (w), 286 (w), 249 (w), 230 (w), 210 (ssh), 191 (s), 176 (s), 158 (m), 146 (w) cm^{-1}. Raman: 3071 (s), 1570 (m), 1443 (w), 1386 (s), 1284 (m), 1172 (w), 1127 (m), 1040 (w), 1022 (s), 1000 (w), 784 (s), 633 (m), 123 (vs), 107 (vs) cm^{-1}. $C_{42}H_{32}Ho_2N_{22}$ (1174.58): calcd. C 42.94, H 2.75, N 26.23; found C 43.1, H 2.9, N 26.1.

X-ray Crystal Structure Determination: The data collections for single-crystal X-ray determinations of **1**, **2**, **3**, and **6** were carried out with an IPDS-II diffractometer (STOE). Structure solutions: SHELXS-86;[48] structure refinements: SHELXL-97.[49] Integrity of symmetry and geometry: PLATON.[50] All non-hydrogen atoms were refined anisotropically. The hydrogen atoms were placed in calculated positions and assigned to an isotropic displacement parameter of 1.2× the size of the isotropic displacement parameter of the referring carbon atom. The crystal of **3** used for data collection shows another small crystalline individual that grows on the surface (RECIPE).[51] The two individuals were separated (TWIN)[52] and refined individually.

The powder samples of compounds **4** and **5** were investigated in sealed capillaries with a Huber Image Foil Guniner Camera 670 diffractometer with a focused single crystal germanium monochromator (Mo-$K_{\alpha1}$ radiation, λ = 0.709300 Å for **4** and Cu-$K_{\alpha1}$ radiation, λ = 1.540598 Å for **5**). Because **4** and **5** decline in their grade of crystallinity upon grinding, samples of both compounds could be made only roughly homogeneous and were investigated in 0.3 mm capillaries, though this led to a higher background due to absorption phenomena of the rare earth atoms. The diffraction patterns of the terbium (**4**) and the ytterbium (**5**) compounds were compared with simulated diffractograms of **1**, **2**, **3**, and **6** and reveal that **3**, **4**, and **5** crystallize isotypically, whereas the powder patterns of **1**, **2**, and **6** are completely different. The cell constants of **4** were refined on 23 reflections, and the best possible resolution leads to a triclinic unit cell without unindexed lines and an average $\delta(2\theta)$ of 0.020° [T = 293(2) K, a = 1019.0(14) pm, b = 1061.3(21), c = 1248.1(21) pm, α = 72.27(13), β = 84.12(14), γ = 78.43(13)°, V = 1258.3(24)$\times10^6$ pm^3]. The cell constants of **5** were refined on 20 reflections with the best possible resolution without unindexed lines and an average $\delta(2\theta)$ of 0.044° [T = 293(2) K, a = 1008.7(9) pm, b = 1068.7(10), c = 1214.6(11) pm, V = 1232.2(12) 10^6 pm^3].[53]

Crystallographic Data for $CeC_{24}H_{17}N_{12}$ (1): monoclinic, $C2/c$, Z = 4, T = 170(1) K, a = 1385.2(3), b = 1789.7(4), c = 1071.5(3) pm, β = 115.90(3)°, V = 2389.7(5)·10^6 pm^3, μ = 19.5 cm^{-1}, Mo-K_α, 4.56 ≤ 2 θ ≤ 59.30°, –6 ≤ h ≤ 18, –24 ≤ k ≤ 24, –12 ≤ l ≤ 13, F(000) = 1212, R_1 = 0.0827 for 1523 reflections [$I > 2\sigma(I)$], R_1 = 0.1313 and wR_2 = 0.1670 for all 2333 unique reflections, GOOF on F_2 = 1.008.

Crystallographic Data for $C_{24}H_{17}N_{12}Pr$ (2): monoclinic, $C2/c$, Z = 4, T = 170(1) K, a = 1382.1(3), b = 1792.8(4), c = 1069.8(3) pm, β = 115.85(3)°, V = 2385.5(5)·10^6 pm^3, μ = 20.1 cm^{-1}, Mo-K_α, 3.98 ≤ 2 θ ≤ 59.26°, –19 ≤ h ≤ 19, –24 ≤ k ≤ 24, –14 ≤ l ≤ 14, F(000) = 1216, R_1 = 0.0526 for 1781 reflections [$I > 2\sigma(I)$], R_1 = 0.1295 and wR_2 = 0.1121 for all 3309 unique reflections, GOOF on F_2 = 0.994.

Crystallographic Data for $C_{24}H_{20}N_{11}Nd$ (3): triclinic, $P\bar{1}$, Z = 2, T = 170(1) K, a = 1034.0(2), b = 1075.0(2), c = 1270.2(2) pm, α =

72.51(3), β = 84.96(3), γ = 78.93(3)°, V = 1320.9(4)·10^6 pm^3, μ = 20.4 cm^{-1}, Mo-K_α, 3.76 ≤ 2 θ ≤ 50.0°, –12 ≤ h ≤ 12, –12 ≤ k ≤ 12, –15 ≤ l ≤ 15, F(000) = 864, R_1 = 0.0779 for 1718 reflections [$I > 2\sigma(I)$], R_1 = 0.2006 and wR_2 = 0.1839 for all 4631 unique reflections, GOOF on F_2 = 0.956.

Crystallographic Data for $C_{42}H_{32}Ho_2N_{22}$ (6): triclinic, $P\bar{1}$, Z = 2, T = 170(1) K, a = 1239.1(3), b = 1294.4(4), c = 1443.0(3) pm, α = 85.43(2), β = 87.81(2), γ = 68.99(2)°, V = 2153.5(4)·10^6 pm^3, μ = 37.1 cm^{-1}, Mo-K_α, 2.82 ≤ 2 θ ≤ 54.60°, –15 ≤ h ≤ 15, –16 ≤ k ≤ 16, –18 ≤ l ≤ 18, F(000) = 1144, R_1 = 0.0593 for 5192 reflections [$I > 2\sigma(I)$], R_1 = 0.1262 and wR_2 = 0.1305 for all 9449 unique reflections, GOOF on F_2 = 0.896.

CCDC-294357 (**1**), -294360 (**2**), -294359 (**3**) and -294358 (**6**) contains the supplementary crystallographic data for this paper. These data can be obtained free of charge from The Cambridge Crystallographic Data Centre via www.ccdc.cam.ac.uk/data_request/cif.

Acknowledgments

We gratefully acknowledge the Deutsche Forschungsgemeinschaft for supporting this work through the two SPP 1166 projects "Hoch- und Tieftemperatursynthesen von Selten-Erd-Elementen mit Aminen" and "Synthese von Selten-Erd-N-Komplexen unter extremen Bedingungen bezüglich Temperatur und Druck", and Prof. Dr. G. Meyer for his generous support.

[1] H. Schumann, *Angew. Chem. Int. Ed. Engl.* **1984**, *23*, 474–492; *Angew. Chem.* **1984**, *96*, 475–493.
[2] H. Schumann, J. A. Meese-Marktscheffel, L. Esser, *Chem. Rev.* **1995**, *95*, 865–986.
[3] W. J. Evans, *Coord. Chem. Rev.* **2000**, *206–207*, 263–283.
[4] R. Kempe, *Angew. Chem. Int. Ed.* **2000**, *39*, 468–494; *Angew. Chem.* **2000**, *112*, 478–504.
[5] W. J. Evans, B. L. Davis, *Chem. Rev.* **2002**, *102*, 2119–2136.
[6] S. Arndt, J. Okuda, *Chem. Rev.* **2002**, *102*, 1953–1976.
[7] K. Dehnicke, A. Greiner, *Angew. Chem.* **2003**, *115*, 1378–1392; *Angew. Chem. Int. Ed.* **2003**, *42*, 1340–1354.
[8] G. Wilkinson, J. M. Birmingham, *J. Am. Chem. Soc.* **1954**, *76*, 6210.
[9] R. G. Hayes, J. L. Thomas, *J. Am. Chem. Soc.* **1969**, *91*, 6876.
[10] K. Müller-Buschbaum, *Z. Anorg. Allg. Chem.* **2005**, *631*, 811–828.
[11] G. B. Deacon, A. Gitlits, B. W. Skelton, A. H. White, *Chem. Commun.* **1999**, 1213–1214.
[12] G. B. Deacon, A. Gitlits, P. W. Roesky, M. R. Bürgstein, K. C. Lim, B. W. Skelton, A. H. White, *Chem. Eur. J.* **2001**, *7*, 127–138.
[13] K. Müller-Buschbaum, *Z. Anorg. Allg. Chem.* **2002**, *628*, 2731–2737.
[14] K. Müller-Buschbaum, C. C. Quitmann, *Inorg. Chem.* **2003**, *42*, 2742–2750.
[15] K. Müller-Buschbaum, *Z. Anorg. Allg. Chem.* **2003**, *629*, 2127–3132.
[16] K. Müller-Buschbaum, C. C. Quitmann, *Eur. J. Inorg. Chem.* **2004**, 4330–4337.
[17] C. C. Quitmann, K. Müller-Buschbaum, *Z. Naturforsch.* **2004**, *59b*, 562–566.
[18] G. B. Deacon, C. M. Forsyth, A. Gitlits, B. W. Skelton, A. H. White, *Dalton Trans.* **2004**, 1239–1247.
[19] C. C. Quitmann, K. Müller-Buschbaum, *Z. Anorg. Allg. Chem.* **2005**, *631*, 1191–1198.
[20] K. Müller-Buschbaum, C. C. Quitmann, *Z. Anorg. Allg. Chem.* **2003**, *629*, 1610–1616.
[21] A. de Cian, M. Moussavi, J. Fischer, R. Weiss, *Inorg. Chem.* **1985**, *24*, 3162.
[22] A. A. Trifonov, M. N. Bochkarev, H. Schumann, J. Loebel, *Angew. Chem. Int. Ed. Engl.* **1991**, *30*, 1149–1151; *Angew. Chem.* **1991**, *103*, 1170–1172.
[23] J. Magull, A. Simon, *Z. Anorg. Allg. Chem.* **1992**, *618*, 81–86.
[24] C. Piguet, A. F. Williams, G. Bernardinelli, J.-C. G. Bünzli, *Inorg. Chem.* **1993**, *32*, 4139–4149.
[25] S. Petoud, J.-C. G. Bünzli, F. Renaud, C. Piguet, K. J. Schenk, G. Hopfgartner, *Inorg. Chem.* **1997**, *36*, 5750–5760.
[26] P. B. Iveson, C. Riviere, D. Guillaneux, M. Nierlich, P. Thuery, M. Ephritikhine, C. Madic, *Chem. Commun.* **2001**, 1512–1513.
[27] L. Natrajan, J. Pecaut, M. Mazzanti, C. LeBrun, *Inorg. Chem.* **2005**, *44*, 4756–4765.
[28] M. Ganesan, C. D. Berube, S. Gambarotta, G. P. A. Yap, *Organometallics* **2002**, *21*, 1707–1713.
[29] T. Dube, D. M. M. Freckmann, S. Conoci, S. Gambarotta, G. P. A. Yap, *Organometallics* **2000**, *19*, 209–211.
[30] T. Dube, S. Conoci, S. Gambarotta, G. P. A. Yap, G. Vasapollo, *Angew. Chem. Int. Ed.* **1999**, *40*, 3657–3659; *Angew. Chem.* **1999**, *111*, 3890–3892.
[31] C. C. Quitmann, K. Müller-Buschbaum, *Z. Anorg. Allg. Chem.* **2004**, *630*, 2422–2430.
[32] C. C. Quitmann, K. Müller-Buschbaum, *Z. Anorg. Allg. Chem.* **2005**, *631*, 564–568.
[33] W. J. Evans, G. W. Rabe, J. W. Ziller, *Inorg. Chem.* **1994**, *33*, 3072–3078.
[34] E. Schaumann in *Hetarene III, Part 4 (Houben-Weyl)*, Georg Thieme Verlag, Stuttgart and New York, **1994**, Vol. E8d.
[35] A. Escande, J. Lapasset, R. Faure, E.-J. Vincent, J. Elguero, *Tetrahedron* **1974**, *30*, 2903–2909.
[36] A. Escande, J. L. Galigne, J. Lapasset, *Acta Crystallogr., Sect. B* **1974**, *30*, 1490–1495.
[37] W. F. Hemminger, H. K. Cammenga, *Methoden der Thermischen Analyse*, Springer Verlag, Berlin Heidelberg New York, **1989**.
[38] K. Müller-Buschbaum, C. C. Quitmann, *Inorg. Chem.* **2006**, in press.
[39] C. C. Quitmann, V. Bezugly, F. R. Wagner, K. Müller-Buschbaum, *Z. Anorg. Allg. Chem*. **2006**, in press.
[40] G. Ostendorp, H. W. Rotter, H. Homborg, *Z. Anorg. Allg. Chem.* **1996**, *622*, 235–244.
[41] J. Weidlein, U. Müller, K. Dehnicke, *Schwingungsfrequenzen II, Nebengruppenelemente*, Georg Thieme Verlag, Stuttgart and New York, **1986**.
[42] S. Hüfner, *Optical Spectra of Transparent Rare Earth Compounds*, Academic Press, New York, **1978**.
[43] R. D. Shannon, *Acta Crystallogr. Sect. A* **1976**, *32*, 751–767.
[44] G. Blasse, B. C. Grabmeier, *Luminscent Materials*, Springer Verlag, Berlin Heidelberg New York, **1994**.
[45] J. Sokolnicki, R. Wiglusz, S. Radzki, A. Graczyk, J. Legendziewicz, *Optical Mater.* **2004**, *26*, 199–206.
[46] BASF Technical Information, *Uvinul Lichtschutzmittel*, EVP 004605 d, **2005**.
[47] UMID, UmweltMedizinischerDienst, *Abschlussbericht zur multizentrischen MCS-Studie*, Bundesamt für Strahlenschutz, Umwelt Bundesamt, **2005**.
[48] G. M. Sheldrick, *SHELXS-97*, Program for the Resolution of Crystal Structures, University of Göttingen, **1997**.
[49] G. M. Sheldrick, *SHELXL-97*, Program for the Refinement of Crystal Structures, University of Göttingen, **1997**.
[50] A. L. Spek, *PLATON-2000*, A Multipurpose Crystallographic Tool, University of Utrecht, **2000**.
[51] *STOE Software Package v.1.16*, *RECIPE*, Program for the Identification of Crystalline Individuals, Wiesbaden, **2001**.
[52] *STOE Software Package v.1.16*, *TWIN*, Program for the Separation of Crystalline Individuals, Wiesbaden, **2001**.
[53] *STOE WINXPOW v.1.04*, Program Package for the Operation of Powder Diffractometers and Analysis of Powder Diffractograms, STOE, Darmstadt, **1999**.

Received: January 6, 2005
Published Online: April 10, 2006

